Journal of Volcanology and Geothermal Research 293 (2015) 25–45

Contents lists available at ScienceDirect

Journal of Volcanology and Geothermal Research

journal homepage: www.elsevier.com/locate/jvolgeores

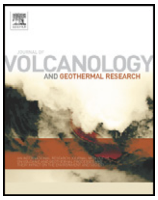

Improved space borne detection of volcanic ash for real-time monitoring using 3-Band method

Y. Guéhenneux *, M. Gouhier, P. Labazuy

Laboratoire Magmas et Volcans, Université Blaise Pascal-CNRS-IRD, OPGC, 5 rue Kessler, 63038 Clermont Ferrand, France

ARTICLE INFO

Article history:
Received 9 June 2014
Accepted 27 January 2015
Available online 7 February 2015

Keywords:
Volcanic ash clouds
MSG-SEVIRI
Infrared data
Real-time monitoring
3-Band method
Optical properties

ABSTRACT

For over 25 years, thermal infrared data supplied by satellite-based sensors are used to detect and characterize volcanic ash clouds using a commonly accepted method: the 2-Band reverse absorption technique. This method is based on a two-channel difference model using the opposite extinction features of water-ice and ash particles at 11 and 12 μm wavelengths. Although quite efficient with the supervision of a user, this method shows however some limitations for reliable automated detection of volcanic ash in a real-time fashion. Here we explore a method dedicated to the operational monitoring of volcanic ash that combines the 11–12 μm brightness temperature difference (BTD_{11-12}) with a second brightness temperature difference between channels 8.7 μm and 11 μm, ($BTD_{8.7-11}$). We first achieve a detailed microphysics analysis of different atmospheric aerosols (volcanic ash, water/ice, sulfuric acid, mineral dust) using optical properties (e.g., extinction efficiency, single scattering albedo and asymmetry parameter) calculated by Mie theory, and showing that $BTD_{8.7-11}$ can be particularly efficient to remove most of artifacts. Then, we tested this method for eight different eruptions between 2005 and 2011 from six different volcanoes (Mount Etna, Piton de la Fournaise, Karthala, Soufriere Hills, Eyjafjallajökull, and Grimsvötn) using data from the Spinning Enhanced Visible and Infrared Imager (SEVIRI) on board Meteosat Second Generation (MSG) geostationary satellite. We show that between 95.6% and 99.9% of ash-contaminated pixels erroneously identified by the BTD_{11-12} method (i.e., artifacts) were detected and removed by the 3-Band method. For all eruptions, the 3-Band method shows a high and constant reliability having a false alarm rate in the range 0.002–0.08%, hence allowing operational implementation for automated detection in case of a volcanic crisis.

1. Introduction

Early detection of volcanic ash clouds has become an important objective for the volcanological community, as well as for civilian and military air space monitoring communities. The main purpose is to reduce to an absolute minimum the hazards posed by volcanic ash drifting into air routes (e.g. Casadevall et al., 1999; Guffanti et al., 2005). Due to the increase of air traffic levels, volcanic ash clouds were predicted to be a major source of risk to aviation (Casadevall, 1994a, 1994b; Casadevall et al., 1996; Miller and Casadevall, 1999; Prata, 2009; Prata and Tupper, 2009). Indeed, the major disruption of air traffic operations associated with the loss of billions of Euros caused by the April–May 2010 eruption of Eyjafjallajökull volcano (Iceland), has first highlighted the importance to establish consistent ash concentration threshold and define safe levels of aircraft engine exposure to ash (IVATF, 2010; Schultz, 2012). Also, this eruptive crisis stressed the need for data and methods allowing early and reliable detection, as well as real-time tracking of ash clouds. These are key parameters for volcanic ash transport and dispersion models (VATD) (e.g., Devenish et al., 2012; Millington et al., 2012; Prata and Prata, 2012).

The aim of this paper is precisely to provide an improved methodology allowing real-time monitoring of volcanic ash cloud drifting in the atmosphere. For this purpose we need to address two main requirements. First, ash particle must be reliably distinguished from other atmospheric aerosols (e.g. water droplet, ice crystals, dust) and ground-based artifacts (e.g. thermal relaxation). Then, ash cloud monitoring must be carried out with a time resolution high enough to allow early detection and dynamic tracking. The 2-Band technique used to detect and characterize volcanic ash (Prata, 1989a, 1989b) is based on a two-channel difference model using the opposite extinction features of water/ice and ash particles at 11 and 12 μm wavelengths. This results on a negative brightness temperature difference for ash particles ($BTD_{11-12} < 0$), while water/ice particles exhibit a positive brightness temperature difference ($BTD_{11-12} > 0$). However some issues related to this method may limit its use for automated detection of volcanic ash in a real-time fashion.

Sensors onboard Low-Earth-Orbit (LEO) satellites such as the Advanced Very High Resolution Radiometer (AVHRR) or Moderate-

---

* Corresponding author at: Laboratoire Magmas et Volcans, 5 rue Kessler, 63038 Clermont-Ferrand cedex, France. Tel.: +33 633 548 785 (mobile).

E-mail address: y.guehenneux@opgc.univ-bpclermont.fr (Y. Guéhenneux).

http://dx.doi.org/10.1016/j.jvolgeores.2015.01.005
0377-0273/© 2015 Elsevier B.V. All rights reserved.

Resolution Imaging Spectroradiometer (MODIS) have widely been used for detecting and mapping volcanic ash particles through their characteristic signal in the thermal infrared, with a high spatial resolution (e.g., Rose et al., 2001; Dean et al., 2003; Tupper et al., 2004). On the contrary, sensors onboard geostationary (GEO) satellites such as MSG-SEVIRI allow volcanic clouds dynamics to be tracked, and their ash content quantified within a typical time resolution of one image every 15 min (e.g., Prata and Kerkmann, 2007; Francis et al., 2012; Labazuy et al., 2012). This makes the use of geostationary satellites mandatory for real-time monitoring purposes, as compared to the low time resolution (2 images a day) of typical LEO satellites. In addition, this has increased our ability to provide accurate inputs for model based simulations and hazard assessment (e.g., Peuch et al., 1999; Kaminski et al., 2011; Folch, 2012).

We present here a method for ash clouds detection based on the 2-Band method (Prata, 1989a, 1989b), and previous work of Pavolonis (2010), Pavolonis and Sieglaff (2010) and Francis et al. (2012) using an additional brightness temperature difference test between channels 8.7 μm and 11 μm, ($BTD_{8.7-11}$). We tested here this methodology for eight different eruptions between 2005 and 2011 from six different volcanoes (Mount Etna, Piton de la Fournaise, Karthala, Soufriere Hills, Eyjafjallajökull and Grimsvötn) using data from MSG-SEVIRI. This sensor provides full-disc images every 15 min, with a 3 × 3 km pixel size at nadir, spanning visible to thermal infrared wavelengths through 12 channels. These characteristics make SEVIRI sensor totally appropriate for the real-time monitoring of ash clouds. For the purpose of our study, we will use specifically the spectral bands centered at 8.7, 11 and 12 μm.

2. Fundamental of volcanic ash detection

2.1. The reverse absorption technique

The 2-Band method proposed by Prata (1989a, 1989b), has long been used to detect ash clouds during, for example, the 1992 eruption of Crater Peak, Mt. Spurr Volcano, Alaska (Rose et al., 2001), the 2001 eruption of Mt. Cleveland, Alaska (Dean et al., 2003), the 24 November 2006 eruption of Mt. Etna, Sicily (Andronico et al., 2009), and during the April–May 2010 Eyjafjallajökull eruption (e.g., Bonadonna et al., 2011; Francis et al., 2012; Labazuy et al., 2012; Prata and Prata, 2012) This method is based on absorption and scattering of the upwelling ground radiance $I_0^+(\tau_i,\mu)$ by particles though their extinction cross section, which mainly varies with composition (complex refractive index), size, shape, incident wavelength, and surface roughness of particles. For a partially transparent plane-parallel ash cloud layer, and ignoring multiple scattering, the irradiance of light is exponentially attenuated from I_0 to I_t following:

$$\frac{I_t}{I_0} \approx \exp(-N_v \sigma_{\text{ext}}(x, m) \Delta Z)$$

where I_t is proportional to the at-sensor radiance, N_v is the number of particles per unit volume, and ΔZ is the vertical ash cloud thickness. The extinction cross section (σ_{ext}) represents the capacity of a given particle of radius (r) at a given wavelength (λ), through its size parameter ($x = 2\pi r/\lambda$), to attenuate the incident light in the direction of propagation (i.e. 0°). This attenuation is strongly related to the composition of a particle through its complex refractive index ($m = n + \chi i$): The real part (n) corresponds to scattering of light (i.e., sidetrack of the wavefront direction) and the imaginary part (χ) stands for the absorption of light (dissipation of the incident energy). Several studies (e.g. Spitzer and Kleinman, 1961; Hale and Querry, 1973; Pollack et al., 1973; Schaaf and Williams, 1973; Volz, 1973; Palmer and Williams, 1975; Wen and Rose, 1994) have pointed out significant differences between silicate, water/ice, and sulfuric acid as well as mineral dust refractive indexes in the infrared domain (Table 1), hence making possible the discrimination of volcanic ash.

2.2. The 2-Band method

Indeed, from the calculation of the extinction cross sections using Mie theory, Prata (1989b) has shown that $\sigma_{ext}(\lambda_{11}) < \sigma_{ext}(\lambda_{12})$ for water and ice particles, while $\sigma_{ext}(\lambda_{11}) > \sigma_{ext}(\lambda_{12})$ for ash particles. Therefore, Planck brightness temperature difference (BTD) between channel 11 and 12 μm, defined as $T(\lambda_{11})–T(\lambda_{12})$, is positive above a cloud of water and/or ice particles while it is negative above a cloud of ash particles. This means that, a simple BTD_{11-12} threshold set at 0 K may theoretically be applied to distinguish ash clouds from water and ice clouds. Several issues regarding ash detection using this method have already been highlighted in the literature and summed up in the next section (Section 2.3). Hereafter (Section 3) we give a detailed microphysics analysis of different aerosols using optical properties calculations, and showing why and how some of these issues can be overcome by using the 3-Band technique.

2.3. Known issues

The 2-Band method suffers well documented limitations (e.g. Simpson et al., 2000; Prata et al., 2001; Yu et al., 2002; Watkin, 2003; Pergola et al., 2004; Pavolonis et al., 2006). We can distinguish between two major types of limitations: [1] those leading to an underestimation of the ash cloud size (missed negative BTD_{11-12} signal) and [2] those which generate an overestimation of the ash cloud size (false negative BTD_{11-12} signal).

Underestimation of ash cloud size may occur:

(1) In moisture rich environments which act to mask the negative BTD_{11-12} (Pavolonis et al., 2006). The water may come directly from the magma, from groundwater beneath the crater, or/and more generally from the humid air training during the growth of the ash cloud (Rose et al., 2001). The wet atmospheric column

Table 1
Optical constants of the complex refractive index ($m = n + \chi i$) for 3 different ash compositions, water, ice, sulfuric acid (75% and 95%), and mineral dust (clay and quartz rich) particles at 8.7,11 and 12 μm wavelengths, with the corresponding source authors.

Aerosol type	λ = 8.7 μm		λ = 11 μm		λ = 12 μm		Authors
	Real (n)	Imaginary (χ)	Real (n)	Imaginary (χ)	Real (n)	Imaginary (χ)	
Ash (basalt: 53% SiO_2)	0.81	0.55	2.22	0.39	1.9	0.14	Pollack et al. (1973)
Ash (andesite: 54% SiO_2)	0.78	0.48	2.16	0.42	1.83	0.13	Pollack et al. (1973)
Ash (rhyolite: 73% SiO_2)	0.78	0.77	1.94	0.22	1.74	0.18	Pollack et al. (1973)
Water	1.27	0.038	1.15	0.097	1.11	0.2	Hale and Querry (1973)
Ice	1.28	0.04	1.09	0.2	1.26	0.41	Schaaf and Williams (1973)
H_2SO_4 (75%)	1.51	0.44	1.47	0.28	1.59	0.23	Palmer and Williams (1975)
H_2SO_4 (95%)	1.55	0.55	1.84	0.46	1.81	0.11	Palmer and Williams (1975)
Mineral dust (clay-rich)	1.19	0.29	1.83	0.2	1.78	0.43	Volz (1973)
Mineral dust (quartz-rich)	0.41	1.83	2.03	0.016	1.46	0.16	Spitzer and Kleinman (1961)